


Cite this: *RSC Adv.*, 2017, 7, 21890

Analysis of partially sulfonated low density polyethylene (LDPE) membranes as separators in microbial fuel cells†

Vikash Kumar,^a Ruchira Rudra,^b Arpita Nandy,^b Subrata Hait ^{*a} and Patit Paban Kundu^{*b}

In the present study, sulfonated low density polyethylenes (LDPEs) in varied molar ratios have been analyzed as separating barriers in microbial fuel cells (MFCs) for bioelectricity production. LDPE sulfonation was performed with chlorosulfonic acid for 7, 15, 30, 45 and 60 minutes which revealed respective degree of sulfonation (DS) results of 9%, 12%, 15%, 10% and 7% in SPE-7, SPE-15, SPE-30, SPE-45 and SPE-60 membranes. Prolonged sulfonation (above 30 minutes) has shown additional sulfone crosslinking formation within the membrane structure, thereby reducing the respective DS in the SPE-45 and SPE-60 membranes. Enhanced membrane properties in terms of water uptake, ion-exchange capacity (IEC) and proton conductivity have been observed with an increasing DS as a result of the incorporated sulfonic acid in the membranes. In succession, respective IEC values of 0.0056, 0.015, 0.048, 0.0087 and 0.0012 meq g⁻¹ and proton conductivities of 2.67×10^{-7} , 3.12×10^{-6} , 4.74×10^{-5} , 2.76×10^{-7} and 2.13×10^{-8} S cm⁻¹ have been observed with the SPE-7, SPE-15, SPE-30, SPE-45 and SPE-60 membranes, where reduced membrane properties in the SPE-45 and SPE-60 membranes were observed with additional sulfone crosslinks being formed in the structure. The casted membranes were assembled as a membrane electrode assembly (MEA) in single chambered MFCs, where a maximum power and current density of 85.73 ± 5 mW m⁻² and 355.07 ± 18 mA m⁻² were observed with the SPE-30 (DS 15%) membrane with an overall ~88.67% chemical oxygen demand (COD) removal in a 30 day run. The employed electrogenic firmicutes showed marked reductions in the overall systemic resistance, depicting the relevance of sulfonated LDPE membranes in MFCs as potent separators for bio-energy conversion.

Received 24th February 2017
Accepted 23rd March 2017

DOI: 10.1039/c7ra02317k

rsc.li/rsc-advances

Introduction

A microbial fuel cell is an electrochemical device that converts supplied chemical energy into electrical energy using microbes as biocatalysts. Bennetto *et al.* were one of the first groups that consistently pursued MFC research in the early 1980s and 1990s.^{1,2} Using different approaches, the advances made in microbial fuel cells have drawn much attention in the area of membrane technology where several studies on alternative polymeric electrolyte membranes (PEMs) and their optimization have been conducted in the last few decades, *e.g.* polystyrene, polyether ether ketone (PEEK), poly(arylene ether

sulfone), phenylated polysulfone, polyphosphazenes, polyimides, polybenzimidazole (PBI) and polypropylene (PP).³⁻⁶ In general, any ion permeable material can function as a barrier and serve as a PEM in fuel cells, but the relative tendencies differ from membrane to membrane. For comparison, Kim *et al.*, in their study, examined different cation-exchange, anion-exchange, and ultra filtration (molecular cut-offs of 0.5, 1, and 3 kilodaltons) membranes to determine their effect in MFC performances.⁷⁻⁹ Likewise, various catholytes with different PEMs have also been examined in dual chamber MFCs.¹⁰⁻¹² As an alternative, Ayyaru *et al.* showed a sulfonated polystyrene-ethylene-butylene-polystyrene (SPSEBS) membrane producing approximately 106.9% higher power density in comparison to Nafion 117 in a single chambered MFC.¹³ In another instance, he demonstrated a sulfonated polyether ether ketone (PEEK) membrane with approximately 55.2% higher power density over the Nafion-117 membrane.¹⁴ In a different study, maximum voltages of 0.676 V and 0.729 V with power densities of 39.2–7.39 mW m⁻² and 57.8–5.5 mW m⁻² have been shown with Nafion and Ralex membranes using *Shewanella putrefaciens* as the biocatalyst.¹⁵ Similarly, different low cost materials have been

^aDepartment of Civil and Environmental Engineering, Indian Institute of Technology, Patna, Bihar, India. E-mail: shait@iitp.ac.in; Fax: +91-612-227-7383; Tel: +91-612-302-8195

^bAdvanced Polymer Laboratory, Department of Polymer Science and Technology, University of Calcutta, India. E-mail: ppk923@yahoo.com; Fax: +91-33-2352-510; Tel: +91-33-2352-510

† Electronic supplementary information (ESI) available. See DOI: 10.1039/c7ra02317k

widely studied to reduce the overall fabrication costs in MFCs *e.g.* earthen pots, ceramics, *etc.*¹⁶ In addition to the numerous researches, different approaches for the enhancement of the membrane characteristics, such as the surface adhesion and hydrophilicity, have also been studied with alternative modifications in polyolefins (*e.g.* by sulfonation, photosulfonation, plasma treatment, radiation grafting *etc.*).^{17–21} Various studies on the surface sulfonation of polyethylene films have been performed using oleum and chlorosulfonic acid in an organic phase solvent.^{22–25} In a study, Whitesides *et al.* have shown carboxylic group incorporations on the surfaces of low density polyethylene films through ATR IR spectroscopy.²⁶ Idage *et al.* have also shown the incorporation of functional groups during the surface sulfonation of HDPE films using X-ray photoelectron spectroscopy.²⁷ During these reactions, the incorporated sulfonic acid molecules have been shown as being active for further reaction and functionalization with other compounds.²⁸

Based on that, here we have demonstrated (a) the sulfonation of LDPE by chlorosulfonic acid at room temperature, and (b) its property enhancements in terms of water uptake, ion exchange capacity (IEC) and proton conductivity. The enhanced properties of the surface sulfonated LDPE moieties have been characterized by Fourier transform infrared spectroscopy (FT-IR) and differential scanning calorimetric (DSC) studies, where the marked differences have been studied in detail in comparison to the pristine LDPE membrane. Owing to their reduced production costs, these sulfonated LDPE membranes have been further examined in single chambered open air MFCs as separating barriers for bio-energy generation using electrogenic mixed firmicutes as biocatalysts.

Result and discussion

Fourier transform infrared (FT-IR) analysis

LDPE sulfonation was carried out with chlorosulfonic acid, where the structural identities of the various functional groups were characterized using FT-IR spectroscopy. This featured major peak differences in the pure and sulfonated LDPE membranes (Fig. 1). The corresponding IR peak intensities in the 1160–1162 cm^{-1} and 1398 cm^{-1} range for the symmetrical and asymmetrical stretching of the constituent S=O bonds of the $-\text{SO}_3\text{H}$ groups were observed in all sulfonated membranes. The relevant peaks at 1030 cm^{-1} revealed the presence of pendent sulfonic groups in the sulfonated membrane structures. With increasing sulfonation duration, increments in these peak intensities were observed in all casted membranes. Relatively, the characteristic peak intensities at 3500–3800 cm^{-1} were observed in all sulfonated membranes, corresponding to the $-\text{OH}$ group stretching. As all these peaks were absent in the pure LDPE membrane, these additional peaks were found due to the sulfonation duration effect on the respective LDPE membranes. The peak intensities near 2912 cm^{-1} and 2846 cm^{-1} (asymmetric and symmetric C–H stretching vibrations involving an entire methyl group) were prominent in the pure LDPE structure. In succession, these were found to deteriorate with increasing sulfonation duration. The peak intensities

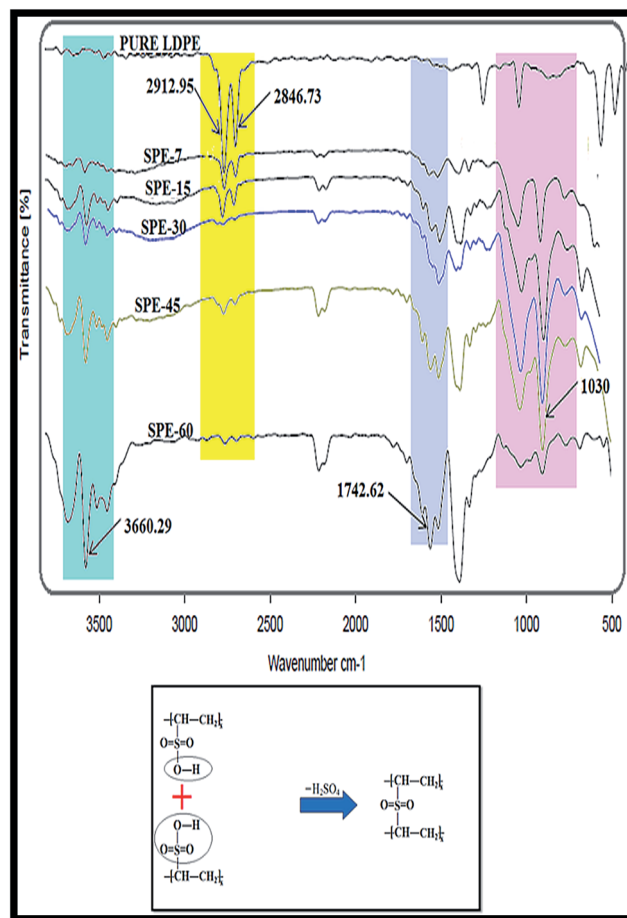


Fig. 1 FT-IR spectra of the membranes (inset: sulfone crosslink formation in the membranes).

diminished evidently with enhanced duration and sulfonate group incorporation in the casted membranes.

In relation, similar but relatively feeble peak intensities were observed with membrane cross sectional analysis. This specifically indicated the increased alkene sulfonic acid formation within the membranes. With increasing sulfonation duration, relative decrements in the corresponding O–H peak stretchings (3500–3800 cm^{-1}) were observed in the SPE-45 and SPE-60 membranes (S1, ESI†). These subliminal O–H peak stretchings with relatively prominent peaks at 1160 cm^{-1} (for the S=O bonds) specifically indicated the presence of the formed sulfone crosslinks (O=S=O) in the SPE-45 and SPE-60 membranes.

This in turn reduced the number of $-\text{OH}$ groups in the SPE-45 and SPE-60 membranes, resulting in feeble peak intensities at 3200–3500 cm^{-1} (in cross sectional membrane analysis). In addition, above 30 minutes, progressive membrane darkening due to excessive sulfonation was observed in the SPE-45 and SPE-60 membranes. These colour changes were indicative of the formed crosslinks that impeded the membrane characteristic peaks.²⁹ The particular peak areas at 1160–1162 cm^{-1} were used for the different sulfonated samples (*X*) and were compared with the obtained area for the pure LDPE membrane (*Y*). From the obtained *X* : *Y* ratio, the degree of sulfonation (DS) for the



different samples was calculated.^{29,30} The obtained degree of sulfonation (DS) values were indicative of the effect of the sulfonation exposure duration on the respective membrane conformity. For the SPE-7, SPE-15, SPE-30, SPE-45 and SPE-60 membranes, respective DS values of 9%, 12%, 15%, 10% and 7% were obtained. In effect, the peak intensities revealed a maximum degree of sulfonation (DS) in SPE-30, whereas for SPE-45 and SPE-60 they disclosed a clear reduction in the DS with membrane darkening due to the extended sulfonation duration (above 30 minutes) that resulted in sulfone crosslink formations in the casted membranes.

Differential scanning calorimetry (DSC) analysis

DSC analysis of the membranes was performed with a differential scanning calorimeter with an empty aluminium pan as a reference. The thermal behaviours of the pure and sulfonated LDPE membranes were analyzed under a temperature range of 30 °C to 150 °C at a constant heating rate of 10 °C per min (Fig. 2). The observed melting temperature of the pure LDPE film was 97.84 °C, but with an increasing degree of sulfonation subsequent reductions in the melting temperatures were observed, e.g. the SPE-30 membrane had a melting temperature of 96.20 °C. However, in the SPE-45 and SPE-60 membranes, further increments in the melting temperatures were observed, which were plausibly due to the formed additional sulfone cross-links that were found to be thermally stable. In addition, the % crystallinity of the membranes was calculated using the equation:

$$X_c = \left\{ \frac{\Delta H_f}{\Delta H_f^*} \right\} / 100 \quad (1)$$

where ΔH_f is the change in the enthalpy of fusion of the polyethylene film, and ΔH_f^* is the standard value for the enthalpy of fusion of the polyethylene film (293.1 J g^{-1}).²⁴ The membrane crystallinity nature was found to be inversely related with the

sulfonation duration, although increments in the % crystallinity of the SPE-45 and SPE-60 membranes were observed due to the formed crosslinks (Table T1, ESI†). The results indicated the effects of sulfonation and crosslinking on the membrane crystallinity properties and melting temperatures. In effect, the formed sulfone crosslinks were found to increase the % crystallinity and melting temperature in the membranes above 30 minutes of sulfonation.

Water uptake and swelling ratio analysis

Sulfonation enhances hydrophilicity and this was clearly observed with the otherwise hydrophobic LDPE membranes that showed relatively increased water retention with an increasing degree of sulfonation. The casted membranes showed respective water uptake (WU) values of 3.24%, 5.43%, 8%, 4.2% and 2.5% for the SPE-7(DS 9%), SPE-15(DS 12%), SPE-30(DS 15%), SPE-45(DS 10%) and SPE-60(DS 7%) membranes (Fig. 3). With an increasing DS, enhancements in the water uptake capacities were observed with the increasing incorporation of sulfonic groups in the membranes. Water absorption prevails *via* hydrogen bond interactions between surface $-\text{SO}_3\text{H}$ groups and water molecules. As a result, the water retention capacity increased within the sulfonated LDPE membranes with increasing sulfonation duration. In relation, marked reductions in the water uptake capacities of the SPE-45 and SPE-60 membranes were observed. These were indicative of the longer sulfonation duration that resulted in additional sulfone crosslinking within the membranes with lower degrees of sulfonation, *i.e.* in the SPE-45 and SPE-60 membranes. These crosslinks in turn lowered the interspace volume of the membranes that showed a comparatively higher % crystallinity and reduced water uptake capacities in the membranes. To rationalize the water uptake results, the swelling properties were calculated. The results followed the same trend as those obtained for the water uptake analysis. Respective swelling ratios (SRs) of 1.5%, 2.8%, 4.1%, 1.8% and 1.1% were observed in the SPE-7, SPE-15, SPE-30, SPE-45 and SPE-60 membranes. A

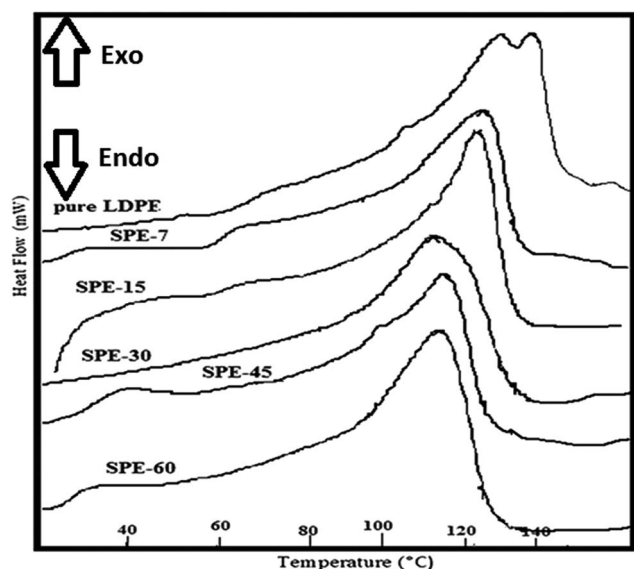


Fig. 2 DSC analysis of the casted LDPE membranes.

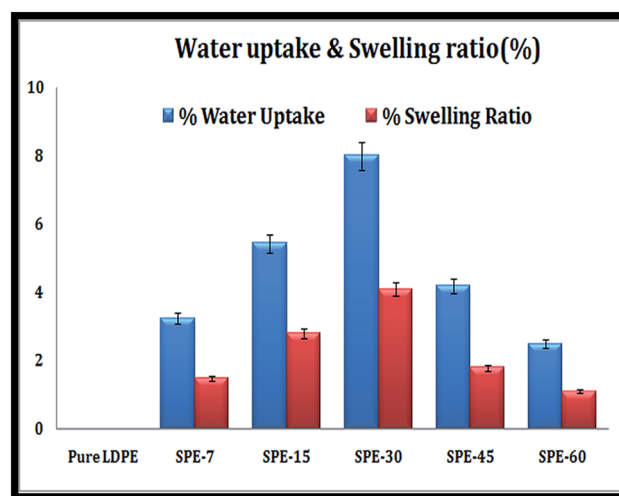


Fig. 3 Water uptake and swelling ratios of the LDPE membranes.



direct correlation existed between the DS and water retention capacity of the membranes, where the sulfonation duration directly influenced the membrane structure with sulfonic group incorporation and crosslink formation. A respective decline in the swelling ratios of the SPE-45 and SPE-60 membranes compared to that obtained for SPE-30 was due to the same aforementioned reason that reduced the water uptake capacities in the membranes. In effect, enhancements in both the parameters in SPE-30 with a higher DS showed its improved qualities over the other casted membranes.

Analysis of IECs and proton conductivity

The membrane ion-exchange capacities (IECs) were calculated through displacement of the initially attached/incorporated ions by an oppositely charged ion present in the surrounding solution.³¹ From titration, respective IECs of 0.0056 meq g⁻¹, 0.015 meq g⁻¹, 0.048 meq g⁻¹, 0.0087 meq g⁻¹, and 0.0012 meq g⁻¹ were obtained for SPE-7, SPE-15, SPE-30, SPE-45 and SPE-60 (Fig. 4).

The values clearly signified the effect of the sulfonation duration, which was the only variable parameter that showed major differences in the ion exchange capacities among the sulfonated and pure LDPE membranes. An initial increase up to 30 minutes was found, with a 30 minute duration giving the optimum result. From thereon, reductions in the IECs were observed in the SPE-45 and SPE-60 membranes. In a similar manner, respective enhancements in the proton conductivity with values of 1.5×10^{-10} S cm⁻¹, 2.67×10^{-7} S cm⁻¹, 3.12×10^{-6} S cm⁻¹, 4.74×10^{-5} S cm⁻¹, 2.76×10^{-7} S cm⁻¹ and 2.13×10^{-8} S cm⁻¹ were observed in the pure LDPE, SPE-7(DS 9%), SPE-15(DS 12%), SPE-30(DS 15%), SPE-45(DS 10%) and SPE-60(DS 7%) membranes. The incorporation of the -SO₃H groups within the membranes was regulated by the sulfonation duration, which eventually aided the transverse protonic conduction. Water molecule interactions with available -SO₃H

groups directly influence the proton conduction *via* a hopping mechanism with hydrogen bond formation.²⁹ With additional formed crosslinks in the SPE-45 and SPE-60 membranes, fewer free -SO₃H groups were available in the membranes with a reduced degree of sulfonation of 10% and 7%. In effect, the crosslinking constricted the interspace volume and hampered the cross sectional ionic mobility in the SPE-45 and SPE-60 membranes. Nevertheless, the obtained results show the positive implications of sulfonation over other membranes through the enhanced membrane properties in terms of the DS, WU, SR, IEC and proton conductivity.

Oxygen diffusivity across the membrane

To study the transverse oxygen diffusivity across the membranes, periodic variations in the dissolved oxygen content were analyzed at the anode. Increased oxygen diffusion from the cathode to anode resulted in respective mass transfer coefficients of 7.8×10^{-6} cm s⁻¹, 1.74×10^{-5} cm s⁻¹, 3.45×10^{-5} cm s⁻¹, 6×10^{-5} cm s⁻¹, 2.1×10^{-5} cm s⁻¹, and 1.2×10^{-5} cm s⁻¹ from the pure LDPE, SPE-7(DS 9%), SPE-15(DS 12%), SPE-30(DS 15%), SPE-45(DS 10%) and SPE-60(DS 7%) membranes (Fig. 5).

Here, a direct correlation with respect to the degree of sulfonation (DS) and oxygen permeability was observed, where the SPE-30 membrane with an increased DS (15%) showed higher oxygen pervasion at the anode. The reason was attributed to the increased intervolumetric spatial structure that allowed more oxygen to diffuse in the chamber. In contrast, SPE-45 and SPE-60, with constricted spacing and formed sulfone crosslinks, showed reduced oxygen permeability in comparison to the SPE-30 membrane. In comparison, approximately 35%, 57%, 63%, 78%, and 87% higher oxygen diffusions were observed in the SPE-60, SPE-7, SPE-45, SPE-15 and SPE-30 membranes over pure LDPE, indicating lower mass transfers (oxygen in-flux) in the SPE-7(DS 9%), SPE-45(DS 10%) and SPE-60(DS 7%) membranes compared with the sulfonated SPE-15(DS 12%) and SPE-30(DS

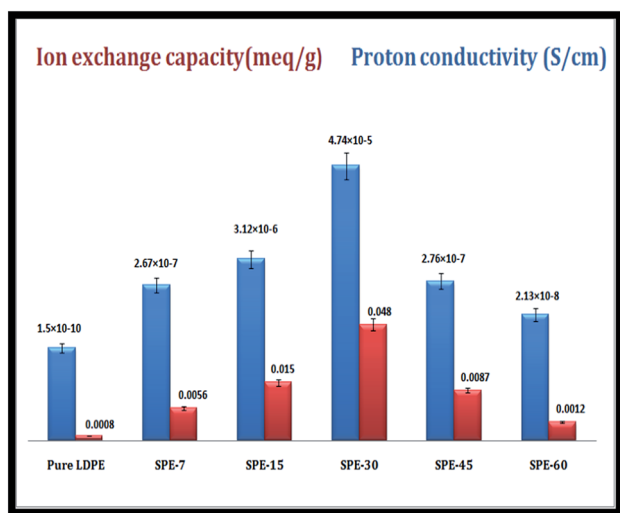


Fig. 4 Ion exchange and proton conductive capacities of the casted membranes.

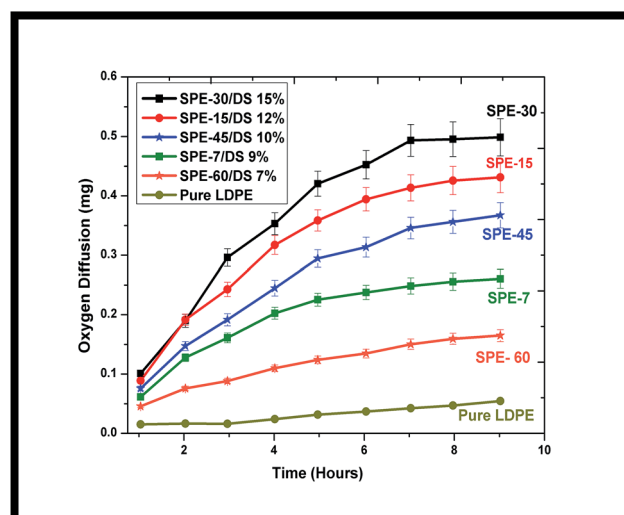


Fig. 5 Oxygen diffusivities across the various casted LDPE membranes.



15%) membranes. Increased oxygen permeation results in direct anolyte oxidation which hampers the overall systemic efficiency. However, taking note of the influence of the LDPE sulfonation, the casted sulfonated membranes were further analyzed as separators in MFCs, utilizing the improved membrane parameters for bio-energy harvesting.

MFC performance

All six MFCs were monitored under similar operating conditions. Initially, the system was kept devoid of external resistances, where the air-facing side of the cathode was masked with parafilm (to establish favourable anodic start-up conditions). With random fluctuations, average anode and cathode potentials of -225 mV and $+171$ mV were observed with Ag/AgCl as the reference electrode (data not shown here). The systems gradually acclimatized with stable OCV (open circuit voltage) increments, where MFC-D (with SPE-30/DS 15%) showed the highest OCV within 10 days of operation. The other MFCs also followed a similar trend but with relatively lower OCV shifts. Maximum open circuit potentials of 301 ± 12 mV, 427 ± 20 mV, 549 ± 30 mV, 611 ± 20 mV, 501 ± 18 mV and 372 ± 15 mV were observed for MFC-A, -B, -C, -D, -E and -F respectively (Fig. 6). With increased voltage drops and currents, MFC-D showed a progressive increase over the other employed units, with all units showing enhanced cell efficiencies with a maximum current of 0.044 mA, 0.128 mA, 0.173 mA, 0.149 mA and 0.086 mA in the respective MFCs (A–F) (S2, ESI†).

This increase relatively indicated the enhanced efficiency of the fitted SPE-30 membrane over other employed membranes. The reason for this was attributed to its higher proton and ionic conductivity with a 15% DS that aided the enhanced performance of MFC-D. In comparison, the SPE-45 (DS 10%) and SPE-60 (DS 7%) membranes with relatively hindered proton conductivities and IECs showed reduced OCVs and currents in MFC-E and -F. This was expected as the formed sulfone

crosslinks reduced the available free sulfonic groups in the SPE-45 and SPE-60 membranes, which were required for relatively higher ionic conductivity. Systemic operations differentiated the performance of the employed membranes in the MFCs. Herein, the MEA was used as an inclusive factor, where close electrode spacing resulted in increased cell efficiencies due to the reduced electrolyte resistance between the electrodes.³² Using this, multiple resistance values (10^7 to 10Ω) in a descending range were employed to obtain MFC polarization curves. Here, increased activation losses with frequent voltage drops were observed at higher resistance (Fig. 7). This was indicative of the energy lost in initiating the redox reaction *i.e.* the charge transfer from the microbe to anode surface. At lower resistance, higher voltage drops were observed, depicting the ease of the electron flow within the circuit. In effect, with SPE-30/DS 15%, the highest power and current densities of 85.73 ± 5 mW m⁻² and 355.07 ± 18 mA m⁻² were observed in MFC-D. Comparatively, respective power and current densities of 9.65 ± 0.5 mW m⁻² and 56.63 ± 3 mA m⁻², 32.65 ± 2 mW m⁻² and 217.36 ± 11 mA m⁻², 56.43 ± 3 mW m⁻² and 288.69 ± 15 mA m⁻², 41.46 ± 2 mW m⁻² and 236.37 ± 12 mA m⁻², and 16.42 ± 0.8 mW m⁻² and 106.63 ± 5 mA m⁻² were observed with MFC-A, -B, -C, -E and -F. Overall, increases in power density of approximately 89%, 53%, 30%, 44% and 69% were observed for MFC-D over the other respective MFCs (A–F). SPE-30, with its relatively higher DS (15%), polarity, IEC and proton conductivity, showed an improved performance over the other fitted membranes. In addition to the single chambered MFC, SPE-30 was further tested in a dual chamber setup, purging pure oxygen at the cathode compartment to ensure its efficacy at higher reduction rates. With pure oxygen available at the cathode, increased power and current densities of ~ 96 mW m⁻² and 372 ± 15 mA

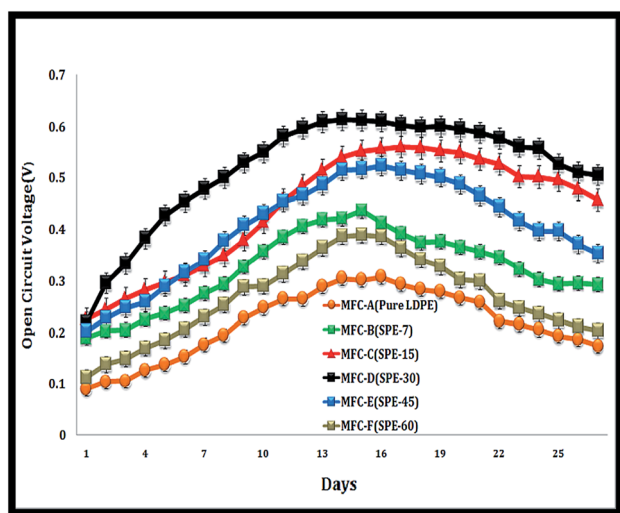


Fig. 6 Open circuit potentials of the MFCs.

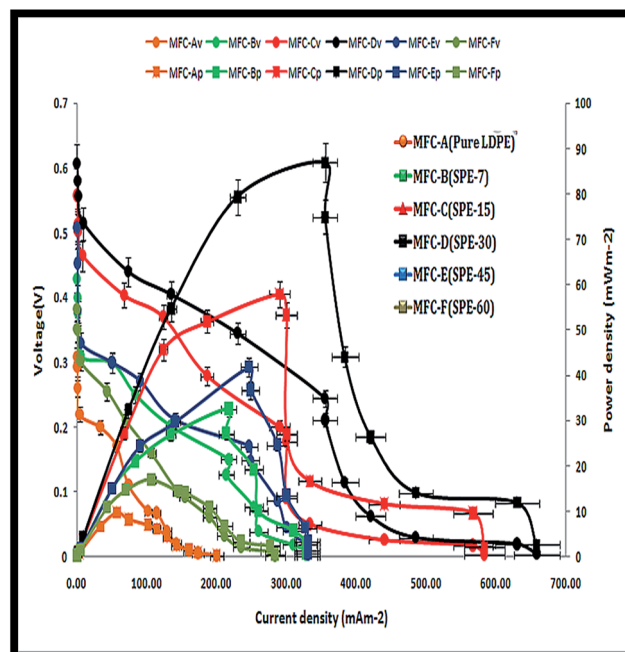


Fig. 7 Polarization curves of the MFCs (V-voltage, P-power density).



m^{-2} were observed for SPE-30 in a dual chamber setup (S3, ESI†).

Although the differences were marginal, the replacement of air with pure oxygen led to a faster reaction at the cathode upon increased oxygen availability. The obtained power output was compared with that from other relevant studies to indicate the effectiveness of sulfonated LDPEs in MFC applications (Table T2, ESI†). In comparison, various lower cost materials (*e.g.* SPEEK/PES, sulfonated PE/poly styrene-DVB) revealed lower power densities with respect to the sulfonated LDPEs employed here, however, other parameters such as the anolyte, microbes and electrode configurations (such as MEAs) were altogether different in these cases. In effect, these thermoplastic insulating low density polyethylenes (LDPEs) were sulfonated not only to achieve hydrophilic channels but also to ensure proton conduction, where the incorporated SO_3^- groups increased the polarity in the inner space of the hydrophobic $-\text{CH}_2$ groups with an increasing DS in the membranes. This served a dual role of proton conduction with electronic charge insulation (electron repulsions) across the membrane. In comparison, the efficiency of the casted sulfonated LDPEs over other lower cost materials was better, as the latter resulted in a reduced efficacy in the system. A logical representation of the system performance with a mixed anolyte substratum has been given in a uniformly accepted way for assessment (ESI† in excel format).³³

Electrochemical impedance spectroscopy (EIS) analysis

Potentiostatic electrochemical impedance spectroscopic (EIS) analysis was performed to measure the internal resistance (R_{in}) of the whole system. The working electrode was connected to the anode, whereas the cathode was connected to the reference and counter terminals. Specific resistive components for each MFC were calculated from the obtained Nyquist graphs (Fig. 8). Additionally, the internal resistance (R_{in}) was segmented into various specific components like activation resistance, ohmic resistance (R_{m} , attributed to the electrode resistance, membrane resistance, *etc.*) and concentration resistance.³⁴

The ohmic resistance (R_{m}) values, as calculated from the equivalent circuit, were $\sim 1754.3 \, \Omega$ for MFC-A, $912.3 \, \Omega$ for MFC-B, $557.6 \, \Omega$ for MFC-C, $296.4 \, \Omega$ for MFC-D, $713.7 \, \Omega$ for MFC-E and $1203.9 \, \Omega$ for MFC-F. Minimal ionic resistance was observed in MFC-D (fitted with SPE-30), where the higher DS (15%) and polarity of SPE-30 allowed increased transverse ionic conduction across the MEA. Significant R_{m} increments from MFC-A to -F were observed, revealing higher membrane impedance due to the increased hindrance in the charge transfer across the membranes.

Nevertheless, it was expected that SPE-15, SPE-7 and pure LDPE, being the least sulfonated and hydrophobic, would show minimal ionic conduction with increased charge transfer resistance. On the other hand, due to the additional cross-linking with relatively lower polarity, IEC and proton conductivity, increased charge transfer interferences were observed in the SPE-45 and SPE-60 membranes. This resulted in a higher impedance in MFC-E and -F. In effect, the lower ohmic resistance in SPE-30 was consistent with the obtained higher

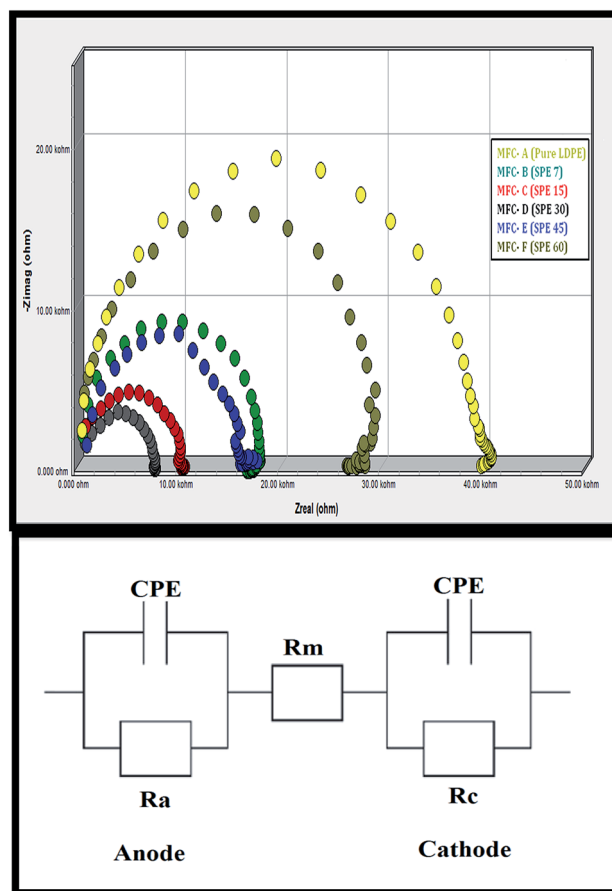


Fig. 8 Electrochemical impedance spectroscopy (EIS) analysis of the MFCs (above), and equivalent circuits representing the ohmic resistance (R_{m}) (below).

efficiency of MFC-D, which was evident of its minimal ionic hindrance in the system.

Microbes and substrate removal

Substrate exhaustion is a natural phenomenon in MFCs and, in order to analyze it, the microbial bio-catalytic activity was evaluated. The outer cell walls of microbes contain exopolysaccharides (EPS) that allow microbial adhesion at the anode surface (carbon cloth fibres). SEM analysis revealed prevailing microbial colonies of the formed biofilms at the anode that bio-catalyzed the electrochemical reactions in the system (Fig. 9). Cyclic voltammetry measurements with repeated potential scans showed prominent microbial redox activities at $887.6 \, \text{mV}$ vs. ref. of $10.54 \, \mu\text{A}$ (oxidation peak), with two distinct reduction peaks at $218.6 \, \text{mV}$ and $-258.3 \, \text{mV}$ vs. ref. of $-10.63 \, \mu\text{A}$ and $-9.54 \, \mu\text{A}$. The electron transfer from the biofilm to the electrode depicted microbial oxidation, whereas the reduction peaks corresponded to microbial reduction (charge transfer from the electrode to the biofilm) in the system. This redox activity was attributed to the microbial cell surface proteins that ensured the electrogenic biocatalytic activity of the employed firmicutes for subsequent substrate utilization upon potentially repeated cycling.



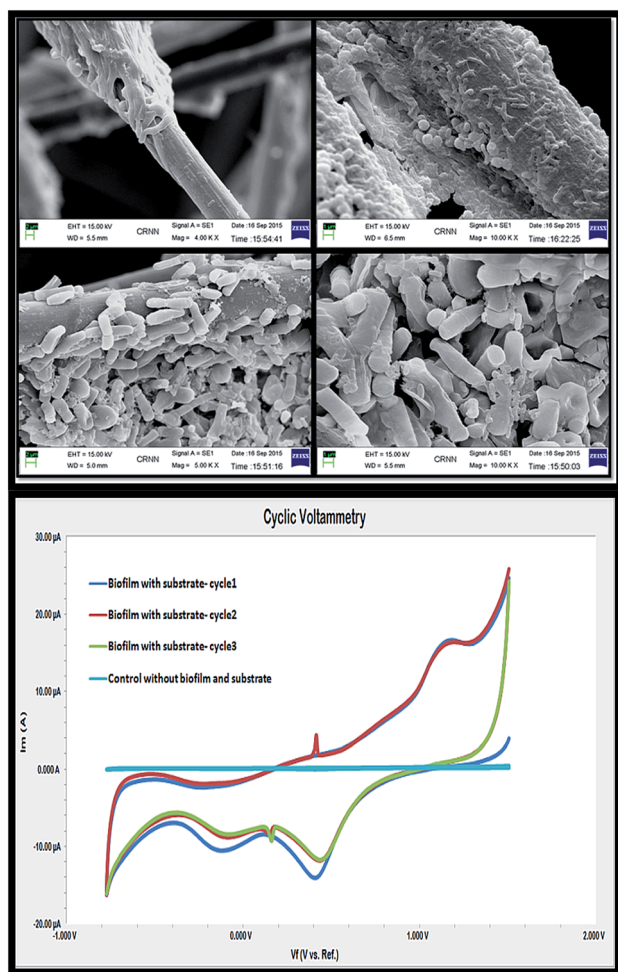


Fig. 9 SEM images of the biofilm on the electrode surface (above), and cyclic voltammograms (below).

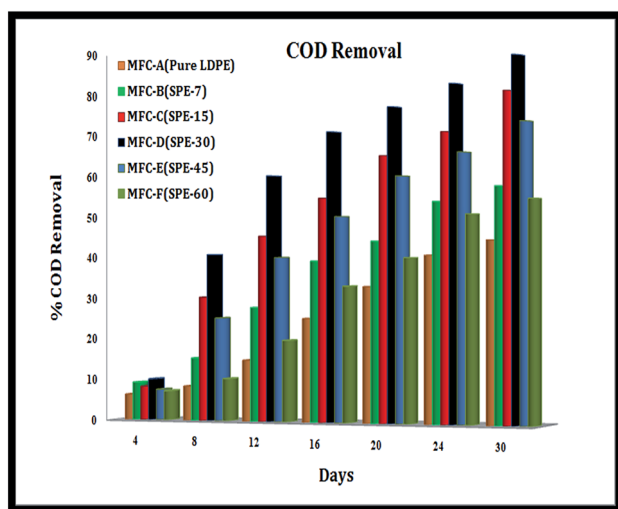


Fig. 10 COD removal of the MFCs.

Overall, respective COD removals of $\sim 44.36\%$, $\sim 57.62\%$, $\sim 80.39\%$, $\sim 88.67\%$, $\sim 73.15\%$ and $\sim 54.27\%$ were observed with MFC-A to F from 150 mg L^{-1} of anolyte in a 30 day run (Fig. 10). These substrate removals were consistent with the systemic performances, which were indicative of the employed individual membranes in the units. MFC-D (with SPE-30/DS 15%), with an increased proton conductive and ion exchange capacity, allowed a higher current to be drawn out of the system and thus showed maximum energy recovery from the unit.

In comparison, the minimal ionic conduction in MFC-A to F resulted in lower current extractions from the system, because of the employed membranes that showed higher cell impedances with comparatively lower DS values, polarities, IECs and proton conductivities. As a result, reduced performances and lower coulombic efficiencies (CEs) were observed in these units (Fig. 11). Sulfonation directly influenced the membrane characteristics where, despite the higher oxygen diffusion, an enhanced coulombic efficiency was observed in the SPE-30 membrane. Comparatively, increases of around 41%, 21%, 5%, 9% and 18% in the CEs were observed in SPE-30 over the pure LDPE, SPE-7, SPE-15, SPE-45 and SPE-60 membranes. Here, the air cathode influenced the cell efficiency with the MEA playing a major role in reducing the overall cell internal resistance with an enhanced CE.^{35,36} Generally, COD removal is largely influenced by the employed membranes and microbes, where it is equally essential to keep them electrogenetically active for sustained substrate utilization. In many cases, the microbial sustenance is adversely affected by charge accumulation at anode, which hampers the anolyte exhaustion with time. Also, the fermentative and methanogenic reactions that predominate in the system limit the microbial metabolism, which affects the overall substrate utilization in MFCs.^{37–40}

Nevertheless, the energy performance corresponded to the successful COD removal and higher CE in the SPE 30 sulfonated LDPE membrane, showing that it is an effective ion exchange barrier for MFC applications. The lower manufacturing costs of

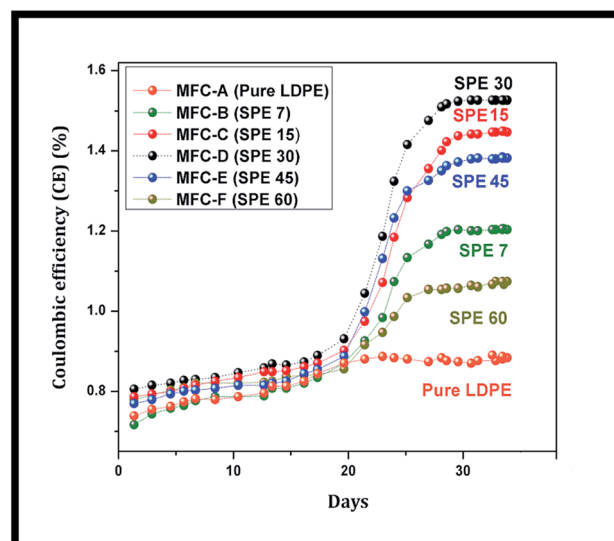


Fig. 11 Coulombic efficiency of the employed LDPE membranes.



the sulfonated LDPE membranes (~ 0.3 \$ per 100 cm²) and their enhanced power generation ability enabled them to be promising separating barriers, where further modifications would robustly enhance their applications in future bio-electrochemical systems and separation fields.

Materials and methods

General conditions

All chemicals used for the experiment were of analytical and biochemical grade. Low density polyethylene (LDPE) was bought from Reliance Polymers, India (22FA002 grade). Chlorosulfonic acid was bought from Merck Millipore, India. Microbiology experiments were performed under strict sterile conditions to avoid contamination.

Preparation of sulfonated low density polyethylene (LDPE) membranes

Low-density polyethylene granules (1.0 g) were compression-molded with a compression load of 1 ton at 200 °C for 15 minutes. The formed membranes (0.22 mm thickness) were treated with chlorosulfonic acid at room temperature for 7, 15, 30, 45 and 60 minutes. Later, these were neutralized with methanol and distilled water. The resulting membranes were named SPE-7, SPE-15, SPE-30, SPE-45 and SPE-60 for the respective 7, 15, 30, 45 and 60 minute sulfonations (Fig. 12).

Furthermore, these obtained membranes were subjected to Fourier transform infrared spectroscopy (FT-IR) and differential scanning calorimetry (DSC) analysis for structural characterization. The degree of sulfonation (DS) values for all of the membranes were calculated from the IR peak intensities using the characteristic $X : Y$ peak ratio (Table 1).²⁹

Water uptake and swelling study

Small pieces of the membranes were kept overnight in deionized water.

The dry and wet weights of the membranes were utilized for the water uptake calculations using the following equation:

$$\text{Water uptake (\%)} = (W_{\text{wet}} - W_{\text{dry}})(100)/W_{\text{dry}} \quad (2)$$

where W_{wet} represents the weight of the wet membranes obtained after soaking in DI water for 24 h, and W_{dry} represents the weight of the respective dry membranes.

Similarly, the swelling ratios of the prepared membranes were calculated from the following equation:

$$\text{Swelling ratio (\%)} = (T_{\text{wet}} - T_{\text{dry}})(100)/T_{\text{dry}} \quad (3)$$

where T_{wet} represents the thicknesses of the wet membranes obtained after soaking in DI water for 24 hours, and T_{dry} is the thickness of the respective dry membranes.

Ion exchange capacity (IEC)

Using the conventional titration method, the ion exchange capacities (IECs) of the respective membranes were determined.

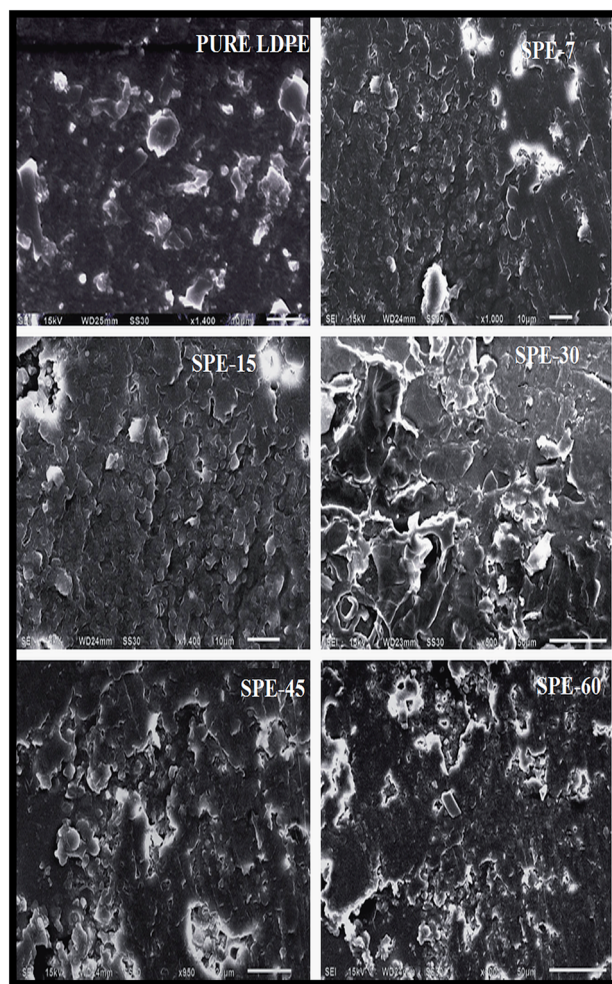


Fig. 12 SEM images of the LDPE membranes.

The membranes were soaked overnight in 1 M H₂SO₄ solution, where excess H₂SO₄ was removed by rinsing with DI water. The samples were then soaked in 50 mL of 1 M NaCl solution overnight, in order to allow replacement of the protons with sodium ions. The remaining solution was titrated with 0.01 N NaOH solution, using phenolphthalein as the indicator. The IEC value (in meq g⁻¹) was calculated using the following equation:

$$\text{IEC} = (V_{\text{NaOH}})(S_{\text{NaOH}})/W_{\text{dry}} \quad (4)$$

Table 1 Membrane characteristics

Sample	Duration of reaction	Degree of sulfonation (%)	% crystallinity
Pure LDPE	—	—	37
SPE-7	7 min	9	35
SPE-15	15 min	12	32
SPE-30	30 min	15	22
SPE-45	45 min	10	35
SPE-60	60 min	7	36



where V_{NaOH} is the volume of NaOH used in the titration, and W_{dry} is the dry weight of the membrane in gm. S_{NaOH} is the strength of NaOH used in the experiment for determination of the IEC.

Proton conductivity

To measure the conductivity of the membranes, AC impedance spectroscopy was employed in the transverse direction at a frequency range of 1 Hz to 10^5 Hz with a 10 mV amplitude (Gamry Reference-600) (S4, ESI†). The conductivities of the samples (σ) were calculated from the Nyquist data, using the following equation:

$$\sigma = T/RA \quad (5)$$

where T is the thickness of the sample, A is the cross-sectional area of the sample, and R is the resistance derived from the lower intercept of the high frequency semi-circle on a complex impedance plane with the real (Z) axis.

Membrane electrode assemblies (MEAs)

Prior to MEA preparation, the membranes were pretreated with a solution mixture of 3 M H_2SO_4 and water (7 : 3). Carbon cloths (6 cm^2) (Zoltek pvt. Ltd, USA) were used as electrodes, which were kept overnight in de-ionized water to remove any unwanted interfacial ionic particle. This also helped in maintaining the electrode's total surface positivity for rigorous microbial attachment. A catalyst mixture of 10 : 90 wt% (Pt/C) with 5% Nafion was sonicated for 30 minutes. The resulting ink was paint coated on the cathode side of the carbon cloth. A total of 3 mg cm^{-2} of supported metal catalyst was loaded onto the air-facing side of the cathode. In total, six sets of sandwiched LDPE membranes (pure LDPE, SPE-7, SPE-15, SPE-30, SPE-45 and SPE-60) between carbon cloth electrodes (as anodes and cathodes) with aluminum sheets were hot pressed at 130°C for 25 seconds at 6.84 MPa pressure. For perfect assembly, these were the optimum conditions, as at higher ranges the fabric became brittle and the carbon cloth lost its texture as an electrode.

Oxygen diffusivity measurement

The mass transfer coefficient k (cm s^{-1}), as characterized by the oxygen permeability, was calculated from the cathode to anode chamber over time using the mass balance equation

$$k^{1/4} = -V/At \ln[C_s - C/C_s] \quad (6)$$

where V is the anode chamber volume, A is the membrane cross-sectional area, C is the anode oxygen concentration, and C_s is the cathode oxygen concentration (assumed to be the saturation concentration of oxygen in water, or 7.8 mg L^{-1}). The oxygen concentrations were measured using a dissolved oxygen probe (Horiba Pvt. Ltd, Kyoto Japan) in the anode chamber. Prior to measurement, the water was purged with purified N_2 gas for the removal of dissolved oxygen and, thereafter, the concentration

of dissolved oxygen was periodically recorded to observe the oxygen diffusivity.

MFC configuration and fabrication

Six identical units, namely A, B, C, D, E and F, with a 150 mL liquid anode volume (with an open air cathode) were fabricated as open air single chambered MFCs, containing pure LDPE, SPE-7, SPE-15, SPE-30, SPE-45 and SPE-60 membranes as the MEAs, respectively (S5, ESI†). The catalyst was loaded onto the air facing side of the cathode facing outwards for oxygen reduction. The other requisite fabrications *e.g.* inlet/outlet sealing, electrode fixing, electrical connections *etc.* were done accordingly to avoid unwanted leakages and errors. These MFC units were sterilized beforehand and filled with de-ionized water for oxygen diffusion studies at the anode. Later, these were subsequently replaced with a microbe enriched anolyte for analysis.

Microbial DNA isolation and gene amplification

The genomic DNA of the microbial strains was isolated using a standard phenol-chloroform method.⁴¹ The universal primers Y1Forward (40th) 5'-TGGCTC AGAACGAACGCGGCGGC-3' and Y2Reverse (337th) 5'-CCCACTGCTGCCTCC CGTAGGAGT-3' were used for 16S rRNA gene amplification *via* polymerase chain reaction (PCR) (Applied Biosystems, US). For microbial species identification, sequencing of the 16S rRNA gene and BLAST tools were employed. These were compared with the allotted accession numbers in the EMBL database. The obtained microbes were firmicute class *Lysinibacillus* species (with the EMBL accession numbers: HE648059, HE648060 and HF548664).

Anolyte preparation

The isolated firmicute class *Lysinibacillus* strains were facultative anaerobes, as they were found to be viable in the cultured anaerobic gas pack jar. These mixed microbial strains were suspended in 50 mM phosphate buffer (50 mL volume) and subsequently transferred to 100 mL of synthetic wastewater ($\sim \text{pH } 6.9$). The COD composition of the feed wastewater was $1800 \pm 240 \text{ mg L}^{-1}$ with a nitrogen total of $114 \pm 27 \text{ mg L}^{-1}$, $\text{PO}_4\text{-P}$ total of $33 \pm 6 \text{ mg L}^{-1}$, and MgSO_4 total of 48 mg L^{-1} . A final volume of 150 mL of the anolyte (with microbe) was used as the feed in the MFCs.

Electrical parameters and measurements

Initially the MFC units were kept under sterilized conditions and filled with de-ionized water at the anode. This was later replaced with a microbial enriched anolyte using a peristaltic pump. For continuous monitoring, a multimeter (Keithley Instruments, Cleveland, OH, USA) and a potentiometer (G600; Gamry Instrument Inc., Warminster, PA, USA) connected with data scanner cards were connected to all of the MFCs *via* a personal computer. The fuel cells were operated continuously for 30 days, where current (I) and potential (V) measurements were recorded after allowing the circuit to stabilize for 8–10



minutes. The power (W) was calculated using the relation $P = IV$, where I and V represent the current and voltage, respectively. The power densities ($mW\ m^{-2}$) were calculated by dividing the obtained power by the anode surface area ($6\ cm^2$).

The substrate removals were analyzed by measuring the chemical oxygen demand (COD) periodically at 420 nm (Anatech Labs India Pvt. Ltd. India), with the measurements being done in triplicate prior to rationalization.

Electrochemical impedance spectroscopy (EIS)

Potentiostatic EIS was performed at a frequency range of 10^3 kHz to 1 mHz (10 mV amplitude) to measure the internal resistance of the unit. Nyquist graphs were plotted and the internal resistance (R_{in}) values were determined for all of the MFCs.³⁴

Cyclic voltammetry (CV)

Cyclic voltammograms at a scan rate of $1\text{--}2\ mV\ s^{-1}$ were analyzed (G600 potentiostat; Gamry Instrument, USA) in order to assess the microbial electrochemical activity. A three electrode setup containing an anode as the working electrode, cathode as the counter electrode, and Ag/AgCl as the reference electrode was used. The reference electrode (Ag/AgCl) was placed near to the anode to minimize the potential iR drop. Furthermore, to ensure the microbial activity, control experiments (without microbes) were conducted separately.

Scanning electron microscopy (SEM)

SEM images were used to analyze the microbial adhesion at the electrode surface. 2.5% glutaraldehyde with 0.1 M phosphate buffer solution was used to fix the biofilm to the anode. Subsequently, it was dehydrated using 30% to 100% ethanol.⁴² The dried samples were sputter coated under vacuum with a thin gold layer. To study the bacterial morphology, a scanning electron microscope (Carl Zeiss EVO® 18 electron microscope) with an acceleration voltage of 15 kV was used.

Conclusion

In summary, sulfonated LDPE membranes with varied sulfonation durations (7, 15, 30, 45 and 60 minutes) were compared as MEAs in single chambered MFCs using mixed electrogenic firmicutes as biocatalysts. Increasing degrees of sulfonation showed improved water uptake, swelling, IEC, proton conductivity and oxygen diffusivity in the membranes. A 30 minute sulfonation (SPE-30) was found to be optimum with an increased degree of sulfonation (15%), and prolonged sulfonation (>30 minutes) resulted in additional sulfone crosslink formation within the membrane structure. This in turn hampered the overall membrane characteristics in prolonged sulfonated membranes, ensuing relatively lower performances in the SPE-45 and 60 membranes. Overall, maximum power and current densities of $85.73 \pm 5\ mW\ m^{-2}$ and $355.07 \pm 18\ mA\ m^{-2}$ were observed with the SPE-30 fitted MFC with minimal internal resistance. Comparing the performance, approximately 89% higher power outputs were observed with the SPE-30 membrane

over the pure LDPE membrane, which clearly showed the direct influence of sulfonation on the naïve LDPE structure. Being a cost efficient material, more LDPE derivatives need to be explored that could potentially serve in large scale energy harvesting processes in future bioelectrochemical applications. MFCs, being a future technology, demand more profound investigations in such diversified areas of membrane technology for relevant cost efficient practical alternatives.

Conflict of interest

The authors declare no competing financial interest.

Acknowledgements

The financial support from the Department of Science and Technology (DST-SERB, Govt. of India) for National Postdoctoral Fellowship (Sanction no – PDF/2016/001018) is duly acknowledged by V. Kumar. The authors also acknowledge Mr Nilkamal Pramanik (Advanced Polymer Laboratory) for the technical and experimental support in DSC analysis.

References

- 1 H. P. Bennetto, J. L. Stirling, K. Tanaka and C. A. Vega, *Biotechnol. Bioeng.*, 1983, **25**, 559–568.
- 2 R. M. Allen and H. P. Bennetto, *Appl. Biochem. Biotechnol.*, 1993, **39**, 27–40.
- 3 H. Zhang and P. K. Shen, *Chem. Rev.*, 2012, **112**, 2780–2832.
- 4 J. Yang, P. K. Shen, J. Varcoe and Z. Wei, *J. Power Sources*, 2009, **189**, 1016–1019.
- 5 L. A. Diaz, G. C. Abuin and H. R. Corti, *J. Membr. Sci.*, 2012, **411–412**, 35–44.
- 6 L. A. Neves, J. Benavente, I. M. Coelho and J. G. Crespo, *J. Membr. Sci.*, 2010, **347**, 42–52.
- 7 Y. Fan, H. Hu and H. Liu, *J. Power Sources*, 2007, **171**, 348–354.
- 8 K. J. Chae, M. Choi, F. F. Ajayi, W. Park, I. S. Chang and I. S. Kim, *Energy Fuels*, 2008, **22**, 169–176.
- 9 J. R. Kim, S. Cheng, S. E. Oh and B. E. Logan, *Environ. Sci. Technol.*, 2007, **41**, 1004–1009.
- 10 K. Rabaey, N. Boon, M. Hofte and W. Verstraete, *Environ. Sci. Technol.*, 2005, **39**, 3401–3408.
- 11 K. Rabaey, P. Clauwaert, P. Aelteman and W. Verstraete, *Environ. Sci. Technol.*, 2005, **39**, 8077–8082.
- 12 K. Rabaey, G. Lissens, S. D. Siciliano and W. Verstraete, *Biotechnol. Lett.*, 2003, **25**, 1531–1535.
- 13 S. Ayyaru, P. Letchoumanane, S. Dharmalingam and A. Stanislaus, *J. Power Sources*, 2012, **217**, 204–208.
- 14 S. Ayyaru and S. Dharmalingam, *Bioresour. Technol.*, 2011, **102**, 11167–11171.
- 15 S. Pandit, S. Ghosh, M. Ghangrekar and D. Das, *Int. J. Hydrogen Energy*, 2012, **37**, 9383–9392.
- 16 M. Behera, P. Jana, T. More and M. Ghangrekar, *Bioelectrochemistry*, 2010, **79**, 228–233.
- 17 H. Wang, S. J. Chen and J. Zhang, *Colloid Polym. Sci.*, 2009, **287**, 541–548.



- 18 M. Kaneko and H. Sato, *Macromol. Chem. Phys.*, 2004, **205**, 173–178.
- 19 M. Kaneko and H. Sato, *Macromol. Chem. Phys.*, 2005, **206**, 456–463.
- 20 M. Kaneko, S. Kumagai, T. Nakamura and H. Sato, *J. Appl. Polym. Sci.*, 2004, **91**, 2435–2442.
- 21 J. Ihata, *J. Polym. Sci., Part A: Polym. Chem.*, 1988, **26**, 167–176.
- 22 D. Fischer and H. Eysel, *J. Appl. Polym. Sci.*, 1994, **52**, 545–548.
- 23 M. Sabne, S. Thombre, S. Patil, S. Patil, S. Idage and S. Vernekar, *J. Appl. Polym. Sci.*, 1995, **58**, 1275–1278.
- 24 M. Kazimi, T. Shah, S. Jamari, I. Ahmed and C. Faizal, *Polym. Eng. Sci.*, 2014, **54**, 2522–2530.
- 25 A. Dimov and M. Islam, *J. Appl. Polym. Sci.*, 1991, **42**, 1285–1287.
- 26 J. Rasmussen, E. Stedronsky and G. Whitesides, *J. Am. Chem. Soc.*, 1977, **99**(14), 4736–4745.
- 27 S. Idage, S. Badrinarayanan, S. Vernekar and S. Sivaram, *Langmuir*, 1996, **12**, 1018–1022.
- 28 J. M. Allan, R. L. Dooley and S. W. Shalaby, *J. Appl. Polym. Sci.*, 2000, **76**, 1865–1869.
- 29 V. Kumar, A. Nandy, S. Das, M. Salahuddin and P. P. Kundu, *Appl. Energy*, 2015, **137**, 310–321.
- 30 J. H. Kim and Y. M. Lee, *J. Membr. Sci.*, 2001, **193**, 209–225.
- 31 J. D. Jeon and S. Y. Kwak, *J. Phys. Chem. B*, 2007, **111**, 9437–9443.
- 32 A. ElMekawy, H. Hegab, X. Dominguez-Benetton and D. Pant, *Bioresour. Technol.*, 2013, **142**, 672–682.
- 33 S. A. Patil, S. Gildemyn, D. Pant, K. Zengler, B. E. Logan and K. A. Rabaey, *Biotechnol. Adv.*, 2015, **33**, 736–744.
- 34 Z. He and F. Mansfeld, *Energy Environ. Sci.*, 2009, **2**, 215–219.
- 35 Y. A. Gallego, X. D. Benetton, D. Pant, L. Diels, K. Vanbroekhoven, I. Genné and P. Vermeiren, *Electrochim. Acta*, 2012, **82**, 415–426.
- 36 X. Zhang, D. Pant, F. Zhang, J. Liu, W. He and B. E. Logan, *ChemElectroChem*, 2014, **1**, 1859–1866.
- 37 A. ElMekawy, H. Hegab and D. Pant, *Energy Environ. Sci.*, 2014, **7**, 3921–3933.
- 38 B. Min, J. Kim, S. Oh, J. M. Regan and B. E. Logan, *Water Res.*, 2005, **39**, 4961–4968.
- 39 Z. He, S. D. Minter and L. T. Angenent, *Environ. Sci. Technol.*, 2005, **39**, 5262–5267.
- 40 J. Greenman, A. Gálvez, L. Giusti and I. Ieropoulos, *Enzyme Microb. Technol.*, 2009, **44**, 112–119.
- 41 A. Ghosh, B. Maity, K. Chakrabati and D. Chattopadhyay, *Microb. Ecol.*, 2007, **54**, 452–459.
- 42 S. Xu and H. Liu, *J. Appl. Microbiol.*, 2011, **111**, 1108–1115.

